IET Intelligent Transport Systems

Special Section: Scientific Seminar of the Italian Association of Transport Academicians (SIDT) 2019

IET Journals
The Institution of Engineering and Technology

Simulation framework for pedestrian dynamics: modelling and calibration

ISSN 1751-956X
Received on 16th October 2019
Revised 30th April 2020
Accepted on 24th June 2020
E-First on 28th July 2020
doi: 10.1049/iet-its.2019.0677
www.ietdl.org

Carlo Liberto[1,2] ✉, Marialisa Nigro[2], Stefano Carrese[2], Livia Mannini[2], Gaetano Valenti[1], Cristiano Zarelli[2]

[1]Laboratory of Systems and Technologies for Sustainable Mobility & Electric Energy Storage, ENEA, via Anguillarese 301, 00123, Rome, Italy
[2]Department of Engineering, Roma Tre University, via Vito Volterra 62, 00146, Rome, Italy
✉ *E-mail: carlo.liberto@enea.it*

Abstract: Pedestrian flow efficiency and safety are primary requirements in the effective configuration and management of urban gathering spaces, such as railway stations, stadiums, or shopping malls. Moreover, the quality and comfort level of available walking environments play a key role in the challenge of sustainable mobility. As a consequence, there has been growing interest in developing methodologies for analysing the walking transport mode. In this context, the authors deem crucial to build a pedestrian dynamics simulation framework that they can completely control, from the modelling and calibration under different flow conditions to the implementation of a user-friendly tool that allows testing the model in a variety of case studies. In this study, they focus on the implementation and calibration of an agent-based model that microscopically simulates the interactions between individuals and with the environment. They calibrate the model parameters with a behavioural-based approach that relies on observed motion behaviours. Additionally, they present preliminary findings from pedestrian flow experiments performed and monitored with dedicated video recording systems. The collected data are meant to improve the calibration and validate the simulator, but they also provide insights into the emergence of collective behaviours, which can have significant upshots on the theoretical framework.

1 Introduction

In modern societies, pedestrian flow efficiency and safety represent key aspects in the effective configuration and management of urban gathering spaces. The growing and pressing necessity of safeguarding pedestrian crowds has been recently tackled with several approaches, such as monitoring of moving people with advanced supervision systems; pro-active management of crowded spaces using real-time decision support systems; automatic detection of anomalous or unexpected behaviours. Concurrently, the research community carried out several efforts attempting to reproduce and predict pedestrian dynamics by means of increasingly advanced computer models and simulation tools.

For several years, the pedestrian flow has been treated with a 'static' approach, introducing general indicators such as level of service [1], regression relationships, and exit systems capacity. However, this approach overlooks the complex collective phenomena related to the microscopic dynamics that are crucial for a realistic representation of pedestrian behaviours (for a complete review refer to [2]). In the early 1990s, Helbing and Molnar laid the groundwork of fluid dynamics-inspired models hypothesising that changes in pedestrian behaviours are driven by social fields and global dynamics can be described through the superposition of attractive and repulsive forces [3]. Various models at different scales have been later proposed to better understand pedestrian dynamics. Examples are represented by microscopic discrete models (such as automaton cell models [4, 5]), microscopic continuous models (such as social force models [6, 7]), behavioural/discrete and activity-based models [8], and network models in which pedestrian flows are described as a queuing network process [9]. Based on these (or similar) models, feature-rich tools have been made available for helping professionals in planning, managing, and designing crowded urban spaces (see e.g. [10–13]). At present, however, these tools are often taken as a closed box. In some cases, modelling parameters are unspecified or inaccessible to the end-user, and the tools are employed for the most diverse applications, even though they had been originally calibrated and validated in *ad hoc* contexts. Frequently, great effort is put into the development of tools with complex high-dimensional models that are even over-parameterised, but then their calibration and validation are underestimated [14, 15]. Finally, despite many models that have been proposed in the literature, there is not yet a universal consensus on the definition of the rules that govern pedestrian flows. A fundamental diagram that faithfully describes the global dynamics might actually not exist at all and, consequently, a complete and accurate understanding of pedestrian behaviours under different conditions is still extremely challenging to achieve.

To tackle these matters with a comprehensive and synergic approach, we undertook a path to build a pedestrian dynamics simulation framework that we can control in every aspect and at each stage, from the modelling and calibration under different flow conditions, to the implementation of a user-friendly tool that allows to test and validate the model in a variety of case studies.

In this paper, we focus on the implementation of the model and its calibration. As a first step, we developed an agent-based model to describe pedestrian motions as a complex system in which behavioural aspects can be decisive for a correct characterisation of the dynamics. Inspired by the Helbing and Molnar's social force model [3], we paid particular attention to the coupled interactions between individuals and with obstacles, investigating innovative elements and, most notably, the predictive ability of human behaviour during the motion. In our assumption, the agent's motion is governed by local information on the surrounding environment, and it is also strongly affected by the agent—and its neighbours—expected future position.

A crucial step is represented by the calibration of the model parameters. This can be carried out with two different, but complementary, approaches behavioural-based and trajectory-driven. The former relies on a heuristic technique that finds a set of optimal parameters from observed behavioural rules of motion, such as the minimum effort and safety distance principles. This calibration methodology relies on the definition and the subsequent minimisation of a multi-objective function that also accounts for conflicting goals [16]. On the other hand, the second approach calibrates the model on the basis of data extracted from real trajectories that can be taken either from the literature or from new, specifically designed, experiments. In this paper, we mainly

developed the first calibration methodology, while we only provide preliminary findings on the second one, since collecting a significant and representative sample of data is time demanding. We started organising a set of experiments at the Engineering Department of 'Roma Tre' University, in which a variable number of students has been involved. Several outflow states have been explored and reliable empirical data, such as flow measurements in specific sections and average travel times, have been collected with a video recording system. It is worth stressing that targeted experiments are not only needed for calibration, but they also improve the theoretical framework providing insights into the emergence of collective behaviours from local interactions.

The paper is organised as follows. In Section 2, we provide a review of the literature concerning the evolution of the social force-based models that inspired our pedestrian simulation framework. Section 3 describes the agent-based model we developed and implemented, while Section 4 presents its calibration following the heuristic approach. An introduction to the first experiments we have been carrying out at 'Roma Tre' University is presented in Section 5. In Section 6, we discuss the simulation framework implemented so far and the planned future developments of this research. Finally, Section 7 summarises our conclusions.

2 State-of-the-art

Many social force-based models have been proposed in the literature and a complete review is outside the scope of this work. However, we proposed a brief history of their evolution, focusing on the most relevant works that have brought significant updates and developments.

Pedestrian crowds have been studied since the 1950s [17], but it was in the 1970s that Henderson for the first time linked the measures of pedestrian flows with the Navier–Stokes equations [18]. These equations are able to describe the behaviour of almost any fluid flow returning a solution in macroscopic terms. This approach was taken up in the 1990s by Helbing who provided a mathematical definition based on the gas-kinetic model (Boltzmann-like model). Specifically, the equations developed by Helbing describe the behavioural changes of individuals according to social fields [3]. In this context, the forces acting on the pedestrian are not classical Newtonian forces and, consequently, the principle of action and reaction is not in force, nor is the law of energy conservation. The novelty is in the introduction of the social forces that are not directly originated by the surrounding environment, but they represent the personal motivation of the pedestrian to react to sensory stimuli, such as the imminent collision with boundaries or neighbours. The stochastic version of the model was then reported in [19] where authors concentrated on the emergence of self-organised spatio-temporal patterns such as the formation of lanes of uniform walking directions and the oscillation of the passing direction through a bottleneck. Then, in [6], authors included in their formulation a body-compression and a sliding-friction term, focusing on panic conditions. They investigated effects such as the uncoordinated motion at high densities, the faster-is-slower effect emerging when people try to escape, and the herding behaviour in finding the exit from a smoky room. A further generalised force model was proposed by Helbing in collaboration with Molnár, Farkas, and Vicsek with the aim to reproduce pedestrian dynamics in both normal and extreme conditions [20]. The model is able to explain several self-organising phenomena and it can also account for panic situations in which clogging and jamming, herding, or fatal pressure can occur. Thanks to these advancements, in a later study, authors combined experiments and simulations in corridors, exits, bottlenecks, and intersections with the purpose to provide guidance for planning pedestrian facilities [21].

In the same year, Lakoba *et al.* [22] explored several values for the social force model parameters and proposed a density-based modification in the definition of the interactions, in order to produce a more realistic behaviour for low-density conditions, preserving the original reliability in the high-density situations. Recently, in [23], an updated and comprehensive review of the social force models was reported, pointing out several model variants, individual attributes, motion base cases, collective and emergent phenomena, and special examples of application. This continuous investigation of pedestrian behaviours led to the development of different simulation models: this is the case of *PEDFLOW* [24], where an agent-based system is implemented in which each individual 'negotiate' its walking space or *NOMAD* [25, 26] where the social force concept is combined with an activity choice approach.

Despite the existence of these and many other models in the literature, as well as their implementation in available simulation tools, it is demonstrated as their usability is dependent on the application for which they were originally developed and calibrated [27]. This is mainly due to the inherent heterogeneity of pedestrian behaviours, which consequently generates the non-existence of a single model able to accurately describe all types of scenarios, as well as a large number of parameters to be set especially in a microscopic representation.

3 Modelling pedestrian behaviours

In this work, we present a model and a simulator that starting from local interactions at the microscopic level can reproduce the emergence of complex behaviours in the pedestrian flows, such as macroscopic structures and global patterns. The model is inspired by the social force concept but, since it is agent-based, each agent can only interact with individuals/obstacles in its neighbourhood and if a high probability of collision exists.

Actually, we have not considered dynamical aspects such as friction and compression [6], group's dynamics [28], temporary attraction areas [29] etc., because for the sake of this work we want to focus on the characterisation and calibration of the one-to-one microscopic interactions among individuals and between individuals and obstacles. Nevertheless, the model will be further developed in order to make it more and more realistic and complex, and in order to include particular features to respond to specific needs.

3.1 Agent-based model

We propose an agent-based system in which each pedestrian is represented by an autonomous entity that observes through 'sensors', acquires information about its surroundings, acts upon the environment and directs its activity towards achieving goals. Specifically, in the perspective of pedestrian dynamic, each agent must be at least able to reach spatial areas—such as an exit door or a station platform—avoiding collisions with neighbours and obstacles—such as columns or walls. In the first version of the model, each agent is described as a circle of radius R between 0.2 and 0.3 m and with speed and acceleration limited, respectively, to 3 and 10 m/s^2.

Inspired by the social force model, behavioural changes in pedestrian dynamics are modelled as reactions to environmental stimuli. The variation of the pedestrian speed is defined in terms of a vectorial quantity that can be interpreted as a social force that reflects a psychological motivation to act. In following its path, each agent tries to keep an individual desired speed, which has been shown to be approximately Gaussian distributed with a mean of 1.4 m/s and a standard deviation of about 0.22 m/s [30]. Any deviation from the desired speed will be compensated through a self-produced acceleration, as given in (3). At the same time, each pedestrian wants to preserve a 'safety' distance from neighbours and obstacles in order to avoid collisions. These interactions are regulated through the definition of a field of view (Fig. 1*a*). Our assumption is that a pedestrian interacts only with neighbours/obstacles he sees and with neighbours/obstacles he can be colliding with. In other words, it is not important where the agent is, but where he is going (Figs. 1*b* and *c*).

3.2 Mathematical formulation

Let us consider an agent i whose position in the plane is identified by the vector $\boldsymbol{r_i} = \boldsymbol{r}(t) = r_x\hat{\boldsymbol{i}} + r_y\hat{\boldsymbol{j}}$ and whose speed at time t is

given by $\boldsymbol{v_i} = \boldsymbol{v}(t) = v_x\hat{\boldsymbol{i}} + v_y\hat{\boldsymbol{j}}$. The rules of the pedestrian behaviour are encoded into the following equations of motion:

$$\begin{cases} \dfrac{\mathrm{d}\boldsymbol{r_i}}{\mathrm{d}t} = \boldsymbol{v_i}(t) \\ \dfrac{\mathrm{d}\boldsymbol{v_i}}{\mathrm{d}t} = \boldsymbol{a_i}(t) + \boldsymbol{\xi_i}(t)\,, \end{cases} \tag{1}$$

which form a stochastic system of coupled Langevin differential equations. $\boldsymbol{\xi_i}(t)$ is a fluctuation term that accounts for random behavioural deviations from the usual rules of motion and it is modelled as a Gaussian white noise. The acceleration is given by

$$\boldsymbol{a_i}(t) = \boldsymbol{a_i^0}(t) + \sum_{j \neq i} \boldsymbol{a_{ij}}(t) + \sum_k \boldsymbol{a_{ik}}(t), \tag{2}$$

where the first term

$$\boldsymbol{a_i^0}(t) = A(\boldsymbol{v}_{\mathrm{des}} - \boldsymbol{v_i}) = A\left(v_i^0 \boldsymbol{e_i^0} - \boldsymbol{v_i}\right) \tag{3}$$

refers to the attraction towards spatial goals (such as exit doors, station platforms etc.) located at $\boldsymbol{r}_{\mathrm{obj}}$. Thus, the larger is the difference between actual speed $\boldsymbol{v_i}$ and desired speed $\boldsymbol{v}_{\mathrm{des}} = v_i^0 \boldsymbol{e_i^0} = v_i^0 (\boldsymbol{r}_{\mathrm{obj}} - \boldsymbol{r_i}) \,/\, \| \boldsymbol{r}_{\mathrm{obj}} - \boldsymbol{r_i} \|$, the higher is the acceleration. In (3), A is a constant parameter that needs to be calibrated.

Although each agent is configured with a pre-set list of spatial goals, its desired direction is dynamically updated to avoid obstacles while minimising the travel distance to the destination. Furthermore, the agent can decide in real-time whether to switch to a competitive goal on the basis of a specific cost function. Currently, this function is defined accounting for both the shortest path and the one that causes fewer changes in the present direction of motion. However, for the future, we are considering updating the function with a time-to-goal estimation based on the local density perception.

Going back to (2) by considering a single couple's interaction, the term in the first sum accounts for collision avoidance from neighbours

$$\boldsymbol{a_{ij}}(t) = \frac{B}{d_{ij}^2}\, \Theta(R_v - d_{ij})\, \Theta\left(\frac{\hat{\gamma}}{2} - |\hat{\gamma}_{ij}|\right) \boldsymbol{p_{ij}} \tag{4}$$

and it is inversely related to the square of the distance between two agents $d_{ij} = |\boldsymbol{d_{ij}}| = |\boldsymbol{r_i} - \boldsymbol{r_j}|$. As expected, this means agent i applies larger avoiding accelerations the closer will be agent j. $\boldsymbol{a_{ij}}$ also depends on the agent field of view, which is defined on the basis of two parameters: the visibility radius R_v and the visibility angle $\hat{\gamma}$ (see Fig. 1*a*). Note that $\hat{\gamma}_{ij}$ is the angle between $\boldsymbol{v_i}$ and $\boldsymbol{r_{ji}} = \boldsymbol{r_j} - \boldsymbol{r_i}$, while Θ is the Heaviside function, which nullifies all the contributions outside the field of view

$$\Theta(x) = \begin{cases} 0, & x < 0 \\ 1, & x \geq 0. \end{cases} \tag{5}$$

The multiplying term $\boldsymbol{p_{ij}} = \boldsymbol{p}(\boldsymbol{r_i}, \boldsymbol{r_j}, \boldsymbol{v_i}, \boldsymbol{v_j}, t_i)$ is the unit vector between the predicted positions of the agents which are going to collide within a certain time $t_i < \tau_{\max}$ (see Fig. 1*b*). In order to identify a collision event, at specific time step t_0, we project the positions of the agents assuming they move with constant speeds and we estimate the time t_i at which the distance between i and j will be equal to the sum of their radii: $d_{ij}(t_0 \leq t_i \leq t_0 + \tau_{\max}) = d_{\mathrm{coll}} = R_i + R_j$. To ensure a certain safety we actually consider $d_{\mathrm{s}} = d_{\mathrm{coll}} + s$, where s can be seen as an extra 'comfort' distance.

Finally, the last sum of (2) accounts for the obstacle-avoidance acceleration due to an obstacle k

$$\boldsymbol{a_{ik}}(t) = \frac{C}{d_{ik}^2}\, \Theta(R_{\mathrm{v}} - d_{ik})\, \Theta\left(\frac{\hat{\gamma}}{2} - |\hat{\gamma}_{ik}|\right) \boldsymbol{p_{ik}}\,. \tag{6}$$

The various terms are very similar to those in (4), the difference is that obstacles are static objects possibly with complex geometries. In this case d_{ik} is the distance between agent i and the nearest point of the intercepted obstacle k and the same reasoning applies to $\hat{\gamma}_{ik}$. It is also worth stressing that we only consider the speed of the agent i itself in the calculation of $\boldsymbol{p_{ik}} = \boldsymbol{p}(\boldsymbol{r_i}, \boldsymbol{r_k}, \boldsymbol{v_i}, t_i)$ and the predominantly direction will be perpendicular to that one that connects the agent and the detected obstacle (see Fig. 1*c*). As before, B in (4) and C in (6) are free parameters of the model.

When more than one agent (obstacle) is detected inside the field of view, there are, at least, two ways in which the acceleration of the ith agent can be estimated. One possibility is to compute the sum of all the pair contributions, each weighted by the corresponding colliding time and/or the corresponding predicted distances [31]. Alternatively, one can estimate the minimum among the colliding times, or among the times of minimum reached distance [32], and then project the positions of the agents in the field of view to that time in order to determine their contributions. Even though we are currently investigating the effectiveness of the different approaches, in this study we decide to adopt the latter as a sort of priority-look-ahead decision rule. In the future, we will also investigate the explicit dependence on t and v of the intensity of the acceleration in (4) and (6).

3.3 Further modelling considerations

As mentioned above (see Section 1), microscopic models can be classified in terms of their representation of space and time. Cellular automaton models take advantage of a discrete

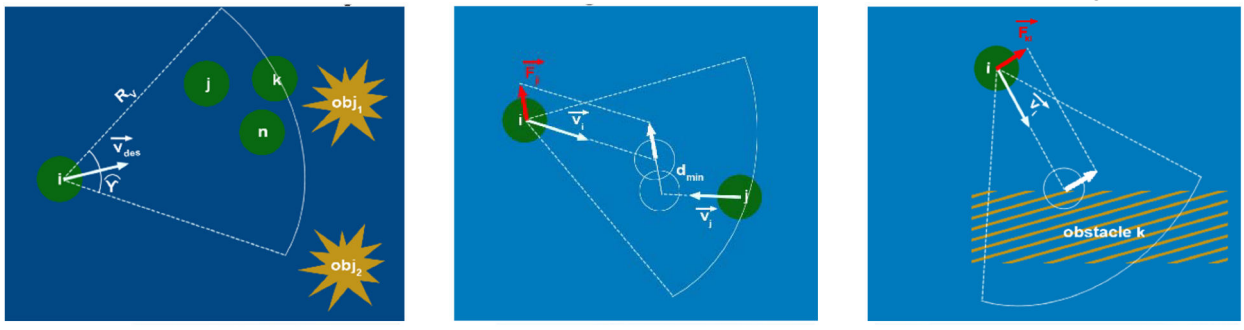

a *b* *c*

Fig. 1 *Field of view. Modelling pedestrian interactions*

(a) Field of view of agent i is identified by the visibility radius R_{V} and a visibility angle γ cantered on the direction of motion of agent i. Each agent moves towards a series of spatial targets (obj_i) with desired speed (v_{des}), ***(b)*** When agent j enters the field of view of agent i, the latter evaluates the probability of an impact based on the foreseen trajectories of motion. If the collision is likely to happen, the pedestrian i applies a 'predictive-avoidance' force, proportional to the inverse of the distance between i and j, ***(c)*** Agents also interact with the surrounding environment and possible obstacles, such as walls or columns. Agent i estimates its probability of impact with an obstacle and, if necessary, it applies a force to avoid it

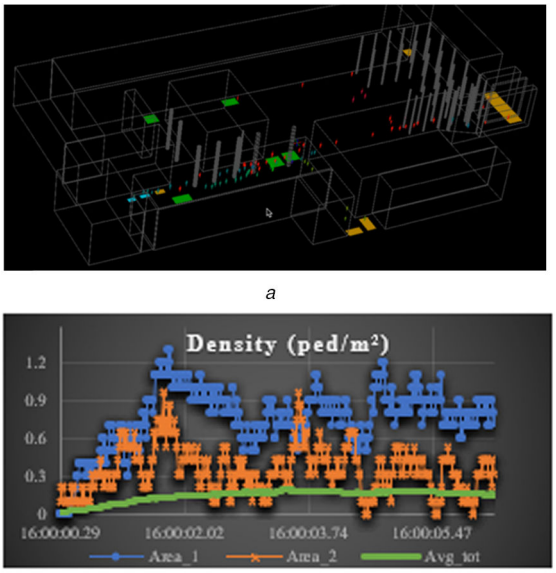

a

b

Fig. 2 *Simulation in complex environment*
(a) Simulation in complex environments (a section of the Tiburtina railway station in Rome. The different colours refer to different walking direction), ***(b)*** Monitoring relevant physical quantities (evolution of density (ped./m^2) for two pre-set zones of the station)

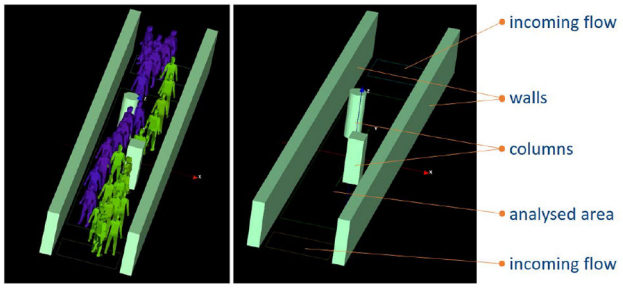

Fig. 3 *Scenario for the calibration process*

representation of space and time to characterise both the environment and the movements within it. In these models, the decision on the next move is determined by the state of the neighbouring cells.

Force models, instead, are microscopic continuous models in which the evolution of pedestrian motion can be expressed in global terms by means of the equations system of (1).

Besides the numerous versions, what really differentiates the models belonging to this category are the pedestrian characteristics and the interaction rules. In the social force model, the general equation describing the interaction between two individuals can be written as

$$\boldsymbol{a_{ij}} = w(\gamma_{ij}(t))\, \boldsymbol{g}(d_{ij}(t)), \tag{7}$$

where γ_{ij} and d_{ij} have the same meaning as in (4) and w is a function able to give more weight to frontal interactions. The function $\boldsymbol{g}$ has been proposed both in the variant 'circular specification' [6], in which it is exclusively dependent on pedestrian positions, and in 'elliptical specifications', where $\boldsymbol{g}$ is defined as the gradient of the repulsive potential

$$\boldsymbol{g} = -\nabla_{b_{ij}}\left(ABe^{-b_{ij}/B}\right), \tag{8}$$

whose equipotential lines have the form of an ellipse pointing in the direction of motion. The semi-minor axis b_{ij} can be defined in terms of either the neighbour's speed v_j: $b_{ij} = f(\tau, d_{ij},\ v_j)$ [3] or the relative pedestrian speeds $v_{ij} = v_j - v_i$: $b_{ij} = f(\tau, d_{ij},\ v_{ij})$ [33]. The elliptical version is commonly implemented in commercial software (e.g. [10]), since it allows to include the 'stride size' τ, i.e. that pedestrians require some free space when moving.

In this paper, we still develop a continuous microscopic model based on the application of behavioural forces, however, different from the aforementioned standard models, the repulsion forces are mathematically defined by a power-law, and the force field itself is shaped by a trajectory forecasting process. In our opinion, predicting trajectories has a significant impact on low and medium density situations in which a long-range interaction can affect pedestrian behaviours. For high-densities conditions, on the other hand, the global dynamics are instead dominated by short-range interactions as well as physical contact forces.

Generally speaking, agent-based models attempt to reproduce some aspects of human behaviours such as the ability to make autonomous decisions and adapt to the environment while achieving goals. As proof of this, in our modelling, each agent is able to dynamically adjust its 'best-path' as a consequence of the obstacles it encounters and to change the local targets by minimising a cost function.

3.4 Implementation

We have implemented the model in a simulator written in Java, including a user-friendly interface that allows us to dynamically change the parameters of the model and to design the simulated environments in a simple way (Fig. 2*a*). Thanks to the simulator, we can perform a 3D rendering of pedestrian flows and define zones where relevant physical quantities, such as the mean density and travel time, can be monitored (Fig. 2*b*).

In the implementation of the model, we numerically solve the system in (1) adopting the Euler method [34]. This is a simple, computationally inexpensive, first-order approximation that allows us to estimate an unknown curve starting from a known initial point of the curve and following the tangent line step by step.

4 Behavioural-based approach for calibrating the model with genetic algorithm

Finding the parameter values that make simulation results as realistic as possible is a complex—much debated—task that plays a fundamental role in building a pedestrian model that can actually be applied to real cases. Despite the lack of a commonly accepted calibration procedure for these types of models [27], we adopt the general methodology similar to that proposed by Campanella *et al.* [16]. It is based on computing the errors between real data and simulation results, usually combined in a multiple-objective function ψ that will then be minimised through an optimisation algorithm. The computation of ψ can be based directly on the capability of the simulator to reproduce real pedestrian trajectories (adoption of microscopic metrics [35]) or to reproduce common aspects of pedestrian behaviour (adoption of macroscopic metrics and/or mesoscopic metrics). Calibration based on the trajectories must take into account the intrinsic stochasticity of the microscopic model and it is to some extent different from calibration on macroscopic or mesoscopic scales [36].

Here, first attempts of calibration tests have been performed on a simple scenario considering a 40×3 m corridor with two obstacles (i.e. two columns, represented as one cylinder of radius = 0.35 m and one parallelepiped of side = 0.7 m, Fig. 3). Different levels of bidirectional flow are simulated in the analysed area defined as a 17 m long section of the corridor, excluding the entrance/exit spaces.

The parameters to be calibrated are A, B, and C values, as reported in (3), (4), and (6), while the view range and view angle have been fixed to 3 m and 2.1 radiant, according to the values from the literature (for a complete analysis of the spatial distribution of the interactions, see [37]). Even though the calibration methodology has currently been applied only for three parameters, the proposed overall approach can be extended to more parameters, as we will progressively increase the model complexity.

We adopted an iterative procedure linking the agent-based simulator with a genetic algorithm (for details on the genetic

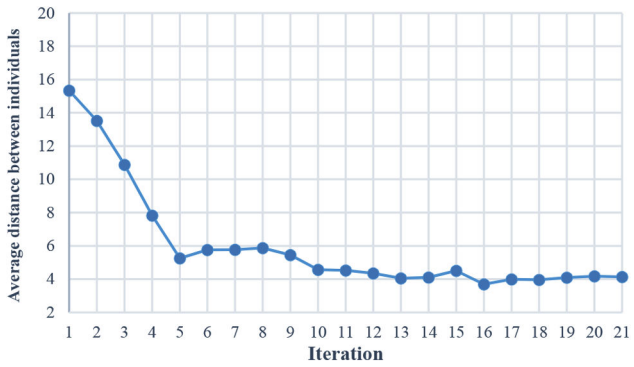

Fig. 4 *Measure of average distance between individuals (i.e. solutions) during genetic algorithm iterations*

Table 1 Average values and standard deviations of the calibrated parameters

Ped. Flow per direction, ped/min	Range	Avg. value, std dev, A, s^{-1}	B, $m^3 s^{-2}$	C, $m^3 s^{-2}$
50	[0–20]	8.27	17.33	4.63
		(3.79)	(2.73)	(0.90)
130	[0–20]	2.10	18.70	6.97
		(0.30)	(1.59)	(4.43)
50	[0–10]	4.67	8.97	4.60
		(2.64)	(0.64)	(1.91)
130	[0–10]	4.10	7.40	5.20
		(3.65)	(0.61)	(3.53)

Corridor with two obstacles, increasing bidirectional flow and two constrained ranges.

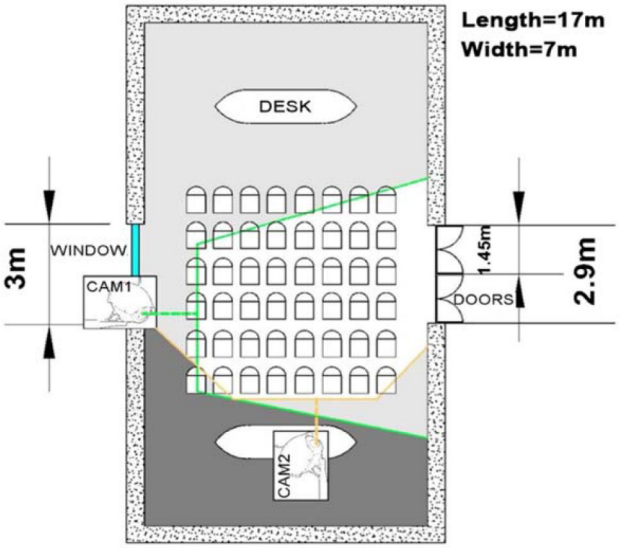

Fig. 5 *Workshop room of the Department of Civil Engineering, Rome Tre University*

algorithm and its settings see the Appendix). Specifically, a multi-objective function has been defined considering the following mesoscopic metrics:

- The number of overlaps between pedestrians.
- The number of overlaps between obstacles and pedestrians.
- The mean absolute difference between the speed of pedestrians and the desired speed.
- The mean absolute difference between the direction of pedestrians and the desired direction.

Thus, the procedure aims to find the best parameters' values in order to keep a safe distance to other pedestrians and obstacles, as well as maximising the travel comfort (least effort principle). Microscopic metrics are not adopted in the present work since the process of collecting a significant sample of data is still in progress (see Section 5).

The algorithm converges to the solutions of the Pareto front, stopping when the population is composed of very similar individuals (Fig. 4).

Concerning the results obtained for the aforementioned scenario of Fig. 3, average parameters' values and their standard deviations are reported in Table 1.

Tests have been conducted for the two different flow conditions of 50 and 130 pedestrians per minute per direction; moreover, the parameters to be estimated have been constrained firstly in the range [0–20], and then in the range [0–10] to reduce the possibility of obtaining unrealistic phenomena.

Considering parameters in the range [0–20] we have relaxed conditions on the upper bounds, which allow the genetic algorithm to search for optimised parameters in a wider domain. Once calibrated, we insert the parameters in (2) and, since in some cases their combination can result in an unrealistic pedestrian acceleration, we also set an upper bound on the total acceleration allowed in the simulator. Results for the range [0–20] showed that A decreases with the increase of pedestrian flow and it oscillates more than the other two parameters B and C, which instead are quite stable.

If the parameters are constrained in the interval [0–10], they are less sensitive to flow changes. In all the tests we carried out, it can be noted how B usually assumes higher values with respect to C. This is probably due to the fact that B is related to the interactions between pedestrians and, in our calibration scenario, these occur more often than interactions with obstacles.

We run these tests mainly to set the integration procedure between the agent-based simulator and the genetic algorithm. Further research is required to (i) set the parameters of the genetic algorithm by performing a sensitivity analysis; (ii) evaluate the differences in the solutions by changing the scenario environment and conditions: it is well known as to obtain a model as generalised as possible to be used in different applications, several scenarios with different settings have to be tested by the calibration process [16]; (iii) introduce in the calibration process additional parameters as the view radius and the view angle, thus progressively increasing the calibration effort.

5 Collecting data with pedestrian flow experiments

We have performed several experimental studies to get a deeper understanding of pedestrian behaviour and crowd dynamics, especially their physical movement and interaction in normal and 'critical' situations. The experimental investigation of pedestrian behaviour is still in progress, thus further insights and evidence are expected to enhance the simulation capability of our pedestrian flow model under different situations and interaction contexts.

Furthermore, the experiments performed help us to test the impact of different environments and boundary conditions on the flow dynamics.

The experiments have been carried out with the collaboration of students of Roma Tre University. The sample consisted of 44 students, of which 18 women and 26 men, with ages ranging from 20 to 30 years old. Thanks to a video recording system we were able to collect empirical data, both quantitative such as densities, flows, and travel times, and qualitative, such as the emergence of patterns and turbulence for intersecting flows, the impact of obstacles along a path, and, more generally, the behaviour and the reaction of involved people. Our experiments have been arranged in the 'workshop room' of the Department of Engineering at Roma Tre University (Fig. 5) and we took advantage of the available chairs to emulate walls and barriers and define several geometric configurations.

Structural elements such as corridors, bottlenecks, intersections, and entry/exit areas are ubiquitous in everyday contexts such as stations, stadiums, cinemas etc. They are particularly relevant in public gathering spaces since they have been proven to give rise to different complex phenomena in the evolution of pedestrian flows and, eventually, to criticalities. This is why their impact is broadly

investigated in the literature (see e.g. [20, 21, 35, 36, 38]) and why we started the experimental study focusing mainly on four configurations:

i. Unidirectional and bi-directional pedestrian streams moving along corridors of different widths with and without a bottleneck under normal situations.
ii. Intersection of multi-directional pedestrian flows in corridors under normal situations.
iii. Evacuation from an anti-panic exit under 'critical' conditions.

The students did not have any knowledge about the final goals or the expected results of the experiments. For the first three interaction contexts, the students were only given initial guidance about the geometrical configuration and were asked to walk at their comfortable walking speed. For the evacuation test, the students were asked to rush towards the exit door when acoustic signals for emergency evacuation was given.

Such experimental contexts have led to a better understanding of how collective behaviour on a macroscopic scale emerges from individual human interactions. However, one has to note that all measurements were performed under well-controlled laboratory conditions.

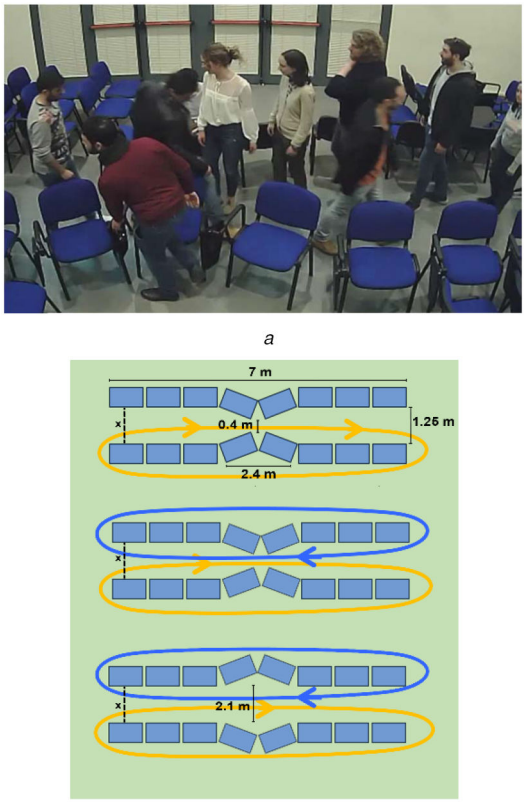

Fig. 6 *Emulating a corridor*
(a) Snapshot from the video recording of the experiment for a bidirectional flow with a bottleneck, ***(b)*** Schematic view of the corridor configurations with bottleneck and enlargement

5.1 Experiments in a corridor

The first experiment we performed refers to a 1.25 m wide corridor in two configurations: with a bottleneck and with an enlargement, and we have considered both unidirectional and bidirectional flows (Fig. 6).

In order to ensure a 'continuous' flow, we asked the participants exiting from one side of the corridor to walk around the chairs and re-enter from the other side. We have compared our findings with results obtained from [21] in a similar experiment, trying to reproduce their setting as closely as possible and we found an overall good agreement (Table 2) with the exception of the case of bidirectional flow with a bottleneck. In this case, they found a higher flow rate and lower time headway between pedestrian with respect to the case of unidirectional flow, observing that bi-directional flows are significantly more efficient than unidirectional flows. They argued this finding is due to better coordination between people who meet each other in opposite directions, as they can react to each other. In contrast, in unidirectional streams, pedestrians do not sufficiently react to what happens behind them and this causes conflicts (e.g. suppressed overtaking manoeuvres) and coordination problems, which reduce the efficiency of motion. However, we were unable to verify this finding. One possible reason is that we used chairs to build corridors, and people involved in the experiment felt them as 'soft' boundaries and people also tried to pass the bottleneck simultaneously from both directions, and there is not an alternation of passing groups in the same direction. This can also be a consequence of the fact that chairs did not obstruct the long-range visibility such as real walls. At the same time, in the mono-directional experiment, most of the students spontaneously decided to get in line, without generating a large number of interactions with neighbours behind them.

5.2 Emergence of uniform walking directions

We have also tested a simple bidirectional flow in a larger corridor (i.e. 3.5 m wide) to verify the emergence of lanes of uniform walking direction, as you can see in Fig. 7. We were able to reproduce this behaviour also with our simulator, where two directional lanes form, as expected from the empirical law proposed in [3]. Our simulator, indeed, allows us to simulate self-organising phenomena that are ubiquitous in nature and in real world walking behaviour, such as ordered patterns that are not induced by initial conditions nor by regulations, but that emerge as a bottom-up process. One of the most studied self-organised pattern is, really, the emergence of lanes of uniform walking directions for bi-directional flows (Fig. 7*b*), or the more general formation of stripes when two streams intersect themselves at a specific angle (Fig. 7*c*). In our experiment, however, sometimes more than two directional lanes appear, and some other times the lanes break. This is also a consequence of the fact that at the end of the corridor people cannot leave but are forced to turn and re-enter the corridor in opposite direction, and this can generate unrealistic effects,

Table 2 Comparison with Helbing *et al.* [3]

	Q	Q_1:Q_2	H_1	σ_1/H_1	H_2	σ_2/H_2
Helbing test						
un. flow (bottleneck)	72	140:0	0.83	0.71	—	—
bi. flow (bottleneck)	87	71:69	1.32	0.62	1.36	0.44
bi. flow (enlargement)	115	69:71	1.05	0.21	0.97	0.24
Our Test						
un. flow (bottleneck)	68	140:0	0.88	0.84	—	—
bi. flow (bottleneck)	59	68:72	2.15	0.49	1.94	0.55
bi. flow (enlargement)	115	73:67	0.98	0.36	1.06	0.46

Q is the overall flow (ped/min) calculated for 140 students and Q_i represent the relative rate of persons for each direction. H_i and σ_i/H_i are, respectively, the mean value of time headways for flow i, and the relative variation of time gaps, both calculated at specific cross-sections x (see Fig. 6*b*).

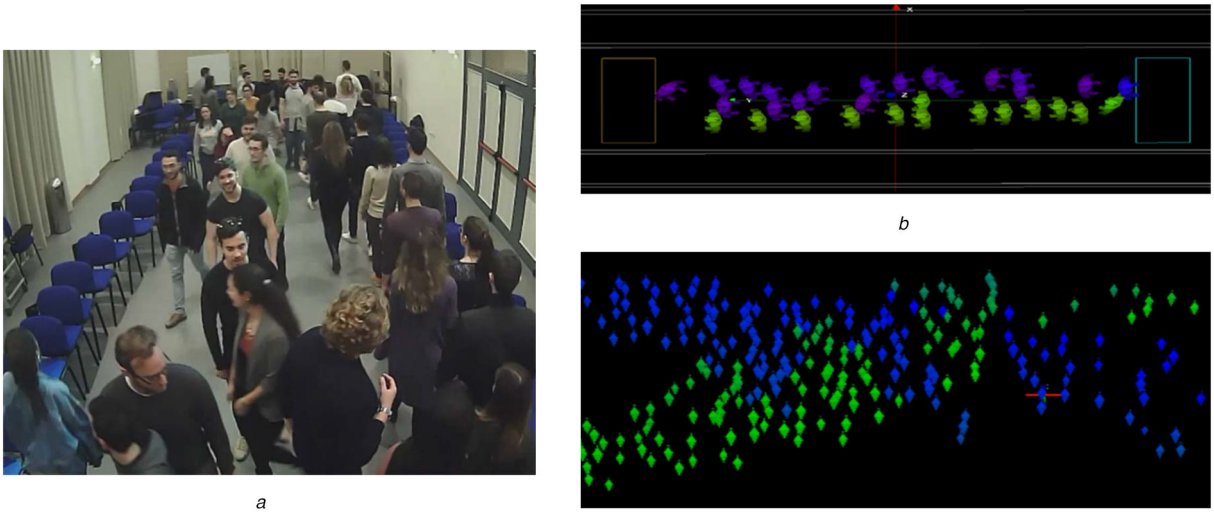

a

b

c

Fig. 7 *Self-organising in lanes of walking direction*

(a) Video recording of the experiment: snapshot of the video for a bi-directional flow in a 3.5 m wide corridor. Lanes of uniform walking direction emerge, ***(b)*** Simulation of counter-flows in a corridor: reproduction of the experiments with the simulator. The average number of lanes is consistent with the relation proposed by Helbing *et al.* [3]: $N(W) = 0.36\,\mathrm{m}^{-1} \times W + 0.59$, where W is the width of the corridor, ***(c)*** Simulation of diagonal intersecting flows: emergence of diagonal stripes at crossing flows: this self-organised phenomenon allows pedestrians to pass through the other stream without having to stop, simply by following the moving sub-stream. The direction of the stripes is orthogonal to the sum of the directions of both intersecting flows

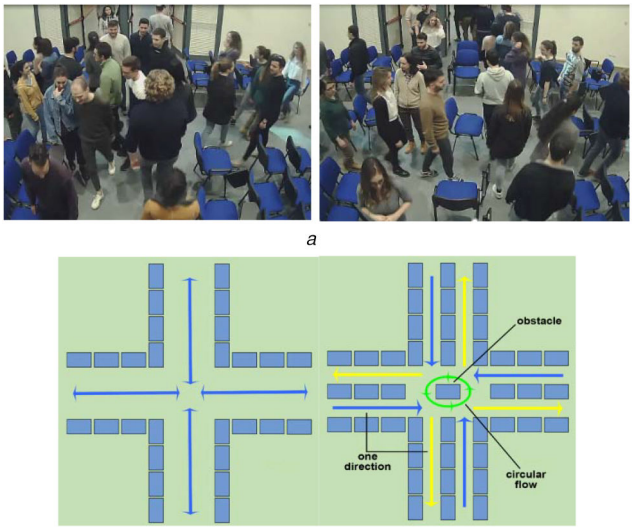

a

b

Fig. 8 *Experiments for intersecting flows*

(a) Snapshots from the video recording of the two experiments, ***(b)*** Configurations for intersecting flows. Related schematic representations of the realised configurations. No regulations in flow directions and no obstacle at the intersection generate unstable flow; by means of 'barriers' and one obstacle at the intersection, a roundabout effect appears and the flow become more efficient

Table 3 Two configurations for intersecting flows

Intersecting flows	No chairs	Chairs
average time, s	7.1	6.7
average distance, m	4.3	5.4
average speed, m/s,	0.6	0.8

Inserting chairs as barriers and one chair as obstacles at the intersection involve the best efficiency and a higher mean speed even though the average travelled distance increase.

partly because of the small spatial extension of our experimental system.

5.3 Experiments for intersecting flows

Another experiment we performed consists of replicating intersecting flows (Fig. 8). First of all, we considered a four-way intersection and, in this configuration, we found that flow is unstable and chaotic. Then, again by means of chairs, we inserted an obstacle in the centre of intersection and barriers to separate flow directions with a one-way regulation.

In this configuration, we found that the flows are more regular and efficient. Indeed, crossing times are shorter and speeds are higher even though a longer average distance is covered by each pedestrian, as a roundabout effect emerges (see Table 3).

Because of the small size of our experimental configuration and the restricted flow rate reached with our sample, we were not able to replicate the emergence of stripes like in [21]. However, our experiment is a simple-but-good example of how to increase the

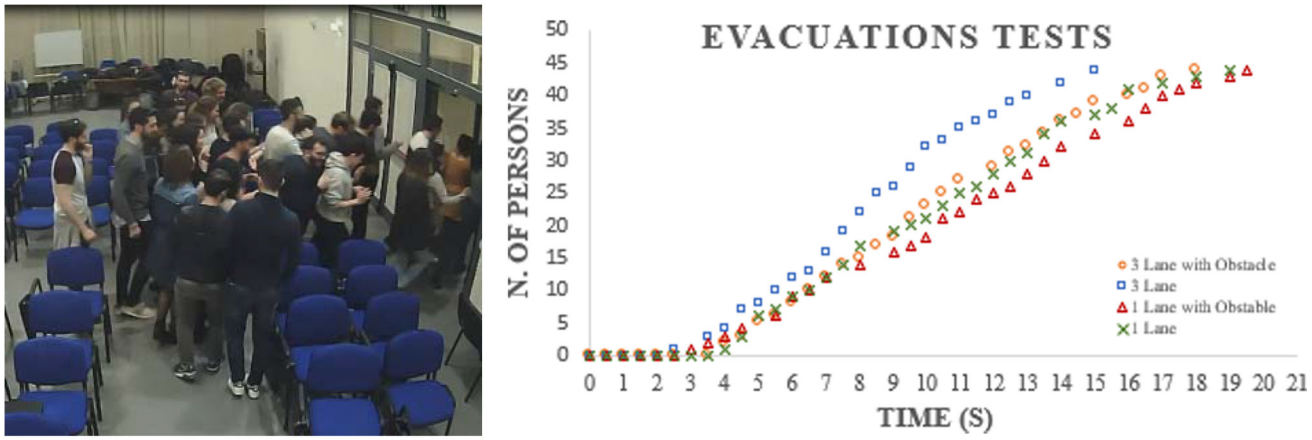

a *b*

Fig. 9 *Evacuation from the exit door*

(a) Video recording of the evacuation test. Snapshot of the evacuation from three different directions without obstacle behind the exit. A minor clogging effect and the formation of an arc-shaped pattern can be observed, ***(b)*** Comparison of evacuation time for the four different configurations

efficiency and safety of pedestrian facilities at comparable costs and even with less available space by means of a simulator. Furthermore, thanks to simulations, one can test several spatial configurations in order to find a skilful flow optimisation. At the same time, simulations can lead to completely unexpected results, since they account for the complex interaction of pedestrian streams that is a consequence of their non-linear dynamics at the microscopic level.

5.4 Tests for evacuation

Finally, we emulate the evacuation of a room through a single exit door (i.e. 1.45 m wide). We explored four configurations: a single and tree-directions flows with and without an obstacle behind the door. The reason for putting an obstacle in front of the exit is that it has been verified that the presence of the obstacle can regularise the flows, break fatal pressures and limit the friction between people [21].

Its functioning is similar to well-known wave breakers since it can absorb pressure in the crowd and reduce the friction level without seriously obstructs the movement toward the exits, as wave breakers. In our experiment, we found comparable evacuation times and similar regular escape (see Fig. 9) for all the cases and the light improvement in the evacuation times goes hand in hand with becoming familiar in repeating the tests. This is likely due to the fact that for safety reasons we could not reproduce an actual situation of panic, with people pushing, falling on the ground, and stepping on each other. Nevertheless, we are planning to extend the worth of this type of experiment, as we will outline in the next section.

6 Discussion and future research

In previous sections, we reported about the theoretical formulation behind the development and the following implementation of an agent-based model able to describe the interactions between individuals and the environment. Observations have to be made about the current reliability and capability of the model, as well as future research needed.

In our model, we focused firstly on the correct reproduction of interactions among individuals and between individuals and obstacles, while contact interactions are not yet represented, and no group's dynamics, nor temporary attraction areas have been considered.

Besides, further modelling improvements will concern the transformation of the agent's circular shape to a more suitable elliptical one and redefinition of the field of view by means of a smoother influence range in which individuals can also react to what is happening closed behind them.

We think that the latter is a wide field of investigation; however, it must be addressed only after a final result in terms of calibration of our base model is achieved.

Our first calibration tests, as reported in Section 4, have been performed by means of a behavioural-based approach combined with a heuristic procedure. This approach has to be fixed with respect to the parameters of the adopted heuristic for several scenarios and conditions.

Moreover, despite its validity, we think that a calibration based on empirical data (trajectory data), rather than a behavioural-based approach, can further improve the results of the calibration process. Actually, as reported in Section 5, several experiments have been conducted to observe flow patterns variations induced by different environmental configurations and to verify some results founded in the literature. The potential of these data, recorded in several videos, is mainly in taking into account the behaviour of people, thus we recognise their usefulness to validate and calibrate the simulator. On the other hand, a first qualitative validation of the model was made by comparing simulations with real motions observed in the videos, and by verifying that the average times detected in the experiments were consistent with those obtained in simulations.

Based on these observations, the current goal of our study is to complete and improve the calibration and validation of the simulator. This can surely benefit from previously collected data, as well as from further experiments with more complex setups (e.g. higher density of people, several floors, stairs, elevators, labs, different exit paths etc.). For what concerns the evacuation tests, we are considering the possibility to repeat the evacuation experiment providing people with protective gears so that we can try and experiment in a more realistic critical situation.

Studying the effect of placing further obstacles along the path to the exits, or simulating unexpected events, such as the malfunctioning of the exit doors, can be also important to verify pedestrian behaviours in real emergency conditions. For example, in panic situations, a pedestrian may lose control, he/she can stumble and step on each other or loses one's bearings. Moreover, in emergency conditions, people get nervous and panic, they lose the ability to act logically and decide on their own. As a result of this lack of independence, people tend to follow others under the assumption they can get them out of danger. Further behavioural aspects may arise such as vanishing of individual personalities and the development of different roles (leaders and followers).

We had not yet the opportunity to measure these behaviours, but we know they will be fundamental for the correct development of a simulator which aim is to improve the safety of public spaces by reproducing pedestrian dynamics. Clearly, these will generate some issues with regard to the experiment setup, i.e. the possibility to observe realistic reactions of the involved people complying with safety regulations and not putting anyone in danger.

Finally, to better highlight the potential of the implemented model and the validity of the proposed approaches, a comparison with well-known models (e.g. [3, 24, 25]) and widely used commercial software (e.g. [10–13]) will be carried out once we complete the calibration of our simulator.

7 Conclusions

We have developed an agent-based model for simulating pedestrian dynamics that we have then implemented in a user-friendly simulator able to represent several complex environments and monitor relevant physical quantities. The formulation we introduced for individual interactions, both between agents and with obstacles, is able to reproduce some well-known emerging collective behaviours, such as the formation of stripes or lanes of uniform walking direction.

We also report the first results on the calibration of the model parameters obtained with a behavioural-based approach. Specifically, we minimised a multi-variable objective function setting up a genetic algorithm; however, further developments are required to constrain the parameters and analyse their variability as a function of the simulated environment.

At the same time, we conducted several pedestrian flow experiments that, aside from being useful for validation and calibration purposes, can show how spatial configurations affect the efficiency of outflows and reveal if we are missing any fundamental aspect in the modelling of pedestrian behaviours. Specifically, our tests for uni- and bi-directional flows in a corridor are in good agreement with results obtained by Helbing *et al.* [21] in all (except one) configurations. Our analysis also confirmed how simple expedients in the design of the intersections may have a significant impact on the overall flow efficiency. Finally, we carried out evacuation tests from an emergency exit which provided us with first indications on the patterns arising from specific environmental configurations and on evacuation times. These latter tests took place in a well-controlled 'laboratory' environment; therefore, they need to be extended to more realistic critical conditions.

This is the first of a series of works targeted to the development of a complete advanced simulation framework of pedestrian dynamics. We hope it can represent a step forward in the understanding of pedestrian behaviours with the final aim of providing a contribution in increasing the efficiency and safety of pedestrian flow dynamics.

8 Acknowledgments

The authors acknowledge funding from the Italian Ministry of Education, University and Research (MIUR), in the frame of the Departments of Excellence Initiative 2018–2022, attributed to the Department of Engineering of Roma Tre University. We are truly thankful to all the colleagues, students, and personnel of Roma Tre University who made the experimental tests possible. Finally, we really thank the reviewers for their comments and suggestions that significantly helped to improve the quality of this paper.

9 References

[1] Fruin, J.J.: '*Pedestrian planning and design*' (Metropolitan Association of Urban and Environment Planners, New York, NY, 1971)

[2] Still, K.: 'Crowd dynamics'. PhD thesis, Mathematics Institute, University of Warwick, UK, 2000

[3] Helbing, D., Molnar, P.: 'Social force model for pedestrian dynamics', *Phys. Rev. E, Stat. Phys. Plasmas Fluids Related Interdiscip. Top.*, 1995, **51**, (5), pp. 4282–4286

[4] Blue, V.J., Adler, J.L.: '*Using cellular automata. Microsimulation to model pedestrian movement*' (Elsevier Science Ltd, Amsterdam, The Netherlands, 1999), p. 114

[5] Dijkstra, J., Jessurun, A.J., Timmermans, H.J.P.: 'A multiagent cellular automata model of pedestrian movement', in Schreckenberg, M., Sharma, S.D. (eds.): '*Pedestrian and evacuation dynamics*' (Springer-Verlag, Berlin, 2001), pp. 173–181

[6] Helbing, D., Farkas, I., Vicsek, T.: 'Simulating dynamical features of escape panic', *Nature*, 2000, **407**, pp. 487–490

[7] Xi, H., Son, Y.-J., Lee, S.: 'An integrated pedestrian behavior model based on extended decision field theory and social force model', Proceedings of the 2010 Winter Simulation Conference, Baltimore, MD, 2010, pp. 824–836, doi: 10.1109/WSC.2010.5679108

[8] Hoogendoorn, S., Bovy, P.: 'Pedestrian route-choice and activity scheduling theory and models', *Transp. Res. B, Methodol.*, 2004, **38**, pp. 169–190

[9] Lovas, G.: 'Modeling and simulation of pedestrian traffic flow', *Transp. Res. B, Methodol.*, 1994, **28**, (6), pp. 429–433

[10] Viswalk: Available at http://vision-traffic.ptvgroup.com/en-us/products/ptv-viswalk, accessed 6 January 2020

[11] LEGION: Available at http://www.bentley.com/en/products/product-line/building-design-software/legion-simulator, accessed 6 January 2020

[12] MassMotion: Available at http://www.oasys-software.com/products/pedestrian-simulation/massmotion, accessed 6 January 2020

[13] Anylogic: Available at http://www.anylogic.com/resources/libraries/pedestrian-library, accessed 6 January 2020

[14] Ciuffo, B., Punzo, V., Montanino, M.: 'Global sensitivity analysis techniques to simplify the calibration of traffic simulation models. Methodology and application to the IDM car-following model', *IET Intell. Transp. Syst.*, 2014, **8**, (5), pp. 479–489,

[15] Montanino, M.: 'Uncertainty management in traffic simulation: methodology and applications'. PhD thesis, University of Naples Federico II, 2014

[16] Campanella, M.C., Hoogendoorn, S.P., Daamen, W.: 'A methodology to calibrate pedestrian walker models using multiple-objectives', in Peacock, R.D., Kuligowski, E.D., Averill, J.D. (Eds.): '*Pedestrian and evacuation dynamics*' (Springer, New York, 2011), pp. 755–759

[17] Hankin, B.D., Wright, R.A.: 'Passenger flow in subways', *Oper. Res. Q.*, 1958, **9**, pp. 81–88

[18] Henderson, L.F.: 'On the fluid mechanics of human crowd motion', *Transp. Res.*, 1974, **8**, (6), pp. 509–515

[19] Helbing, D., Molnár, P.: 'Self-organization phenomena in pedestrian crowds', in Schweitzer, F. (ed.): '*Self-organization of complex structures: from individual to collective dynamics*' (Gordon and Breach, London, UK, 1997), pp. 569–577

[20] Helbing, D., Farkás, I.J., Molnár, P., *et al.*: 'Simulation of pedestrian crowds in normal and evacuation situations', in Schreckenberg, M., Sharma, S.D. (eds.): '*Pedestrian and evacuation dynamics*', (Springer, Berlin, Germany, 2002), pp. 21–58

[21] Helbing, D., Buzna, L., Johansson, A., *et al.*: 'Self-organized pedestrian crowd dynamics: experiments, simulations, and design solutions', *Transp. Sci.*, 2005, **39**, (1), pp. 1–24

[22] Lakoba, T.I., Kaup, D.J., Finkelstein, N.M.: 'Modifications of the Helbing–Molnar–Farkas–Vicsek social force model for pedestrian evolution', *Simulation*, 2005, **81**, (5), pp. 339–352

[23] Chen, X., Treiber, M., Kanagaraj, V., *et al.*: 'Social force models for pedestrian traffic – state of the art', *Transp. Rev.*, 2018, **38**, (5), pp. 625–653

[24] Willis, A., Kukla, R., Hine, J., *et al.*: 'Developing the behavioural rules for an agent-based model of pedestrian movement'. Twenty-fifth European Transport Congress, Cambridge, UK, 2000

[25] Hoogendoorn, S.P., Bovy, P.H.L., Daamen, W.: 'Microscopic pedestrian wayfinding and dynamics modelling', in Schreckenberg, M., Sharma, S.D. (eds.): '*Pedestrian and evacuation dynamics*' (Springer, Berlin, Germany, 2002), pp. 123–154

[26] Hoogendoorn, S.P., Daamen, W., Bovy, P.H.L.: 'Microscopic pedestrian traffic data collection and analysis by walking experiments: behaviour at bottlenecks', in Galea, E.R. (ed.): '*Pedestrian and evacuation dynamics 2003*' (CMS Press, London UK, 2003), pp. 89–100

[27] Porter, E., Hamdar, S.H., Daamen, W.: 'Pedestrian dynamics at transit stations: an integrated pedestrian flow modelling approach', *Transportmetrica A, Transp. Sci.*, 2018, **14**, (5–6), pp. 468–483

[28] Garrett, B., Annunziato, M., Pannicelli, A., *et al.*: 'Modeling crowd motion using swarm heuristics and predictive agents'. 2nd European Symp. on Nature-inspired Smart Information Systems, NiSIS, 2006

[29] Kwak, J., Jo, H.-H., Luttinen, T., *et al.*: 'Effects of switching behavior for the attraction on pedestrian dynamics', *PLOS ONE*, 2015, **10**, (7), p. e0133668

[30] Daamen, W.: 'Modelling passenger flows in public transport facilities'. PhD thesis, Delft University of Technology, Delft, 2004

[31] Annunziato, M., Liberto, C., Pannicelli, A.: 'Modellazione ad agenti dei flussi passeggeri in una stazione di trasporto metropolitano'. Proc. WIVA3, Siena, Italy, 2006

[32] Zanlungo, F., Ikeda, T., Kanda, T.: 'Social force model with explicit collision prediction', *Europhys. Lett.*, 2011, **93**, p. 68005

[33] Johansson, A., Helbing, D., Shukla, P.K.: 'Specification of the social force pedestrian model by evolutionary adjustment to video tracking data', *Adv. Complex Syst.*, 2007, **10**, (2), pp. 271–288

[34] Malham, S., Wiese, A.: 'An introduction to SDE simulation'. arXiv:1004.0646, math, 2010. Available at https://arxiv.org/abs/1004.0646, accessed 10 October 2019

[35] Hoogendoorn, S.P., Daamen, W.: 'A novel calibration approach of microscopic pedestrian models', in Timmermans, H. (ed.): '*Pedestrian behavior: Models, data collection and applications*' (Emerald Group Publishing Limited, Bingley, UK, 2009), pp. 195–214

[36] Sparnaaij, M., Duives, D.C., Knoop, V.L., *et al.*: 'Multiobjective calibration framework for pedestrian simulation models: a study on the effect of movement base cases, metrics, and density levels', *J. Adv. Transp.*, 2019, **2019**, Article ID 5874085, 18 pages

[37] Duives, D.C.: 'Analysis and modelling of pedestrian movement dynamics at large-scale events'. PhD thesis, Delft University of Technology, 2016

[38] Das, S., Manski, C.F., Manuszak, M.D.: 'Walk or wait? An empirical analysis of street crossing decisions', *J. Appl. Econ.*, 2005, **20**, (4), pp. 529–548

[39] Mitchell, M.: '*An introduction to genetic algorithms*' (MIT Press Cambridge, MA, USA, 1998), ISBN: 0262631857

10 Appendix

10.1 Genetic algorithm

The implemented genetic algorithm is based on the following common structure [39]:

- Starting population generation: each member (chromosome) of the starting population has a genome composed of a number of elements equal to the number of variables to be found. At the first iteration, a number of chromosomes (N_C) are randomly created considering for each element of the genome a value for the parameters A, B, and C in the defined constraint intervals (in our tests [0 10] or [0 20]).
- Solutions evaluation: each chromosome is evaluated, performing an agent-based simulation and collecting position, speed and acceleration for each agent every time step (0.05 s).
- Elitism: at each iteration, a percentage value p_{el} of the chromosomes belonging to the population of the previous iteration is sent directly to the population of the next iteration without changes. The elitism starts from the second iteration of the algorithm and the chromosome candidates to this operation are the best ones according to the multi-objective function minimisation.
- Mutation: the mutation is carried out on a percentage value p_m of the chromosomes in all iterations; the chromosomes to be mutated are randomly extracted from those remaining as a result of the elitism. The mutation chooses randomly a direction and step length that satisfies bounds and linear constraints for each element of the genome of the chromosomes entering in the mutation process with respect to the last successful or unsuccessful generation (adaptive feasible mutation);
- Selection: a tournament selection process is adopted;
- Crossover: a scattered crossover is applied between each pair of chromosomes derived from the selection phase, in order to generate a number of new chromosomes equal to percentage value p_{cross} of the starting population.

The starting values of the genetic algorithm have been set according to a population of 50 individuals, while values of p_{el}, p_m, and p_{cross} have been set to, respectively 5, 20, and 80%.